Eur. Phys. J. B **43**, 529–541 (2005)
DOI: 10.1140/epjb/e2005-00087-5

THE EUROPEAN PHYSICAL JOURNAL B

Mesoscopic full counting statistics and exclusion models

P.-E. Roche[1,2,a], B. Derrida[3], and B. Douçot[4]

[1] Centre de Recherches sur les Très Basses Températures, Laboratoire du CNRS, associé à l'Université Joseph Fourier, 25 avenue des Martyrs, 38042 Grenoble Cedex 9, France
[2] Laboratoire Pierre Aigrain, École Normale Supérieure, 24 rue Lhomond, 75231 Paris Cedex 05, France
[3] Laboratoire de Physique Statistique, École Normale Supérieure, 24 rue Lhomond, 75231 Paris Cedex 05, France
[4] Laboratoire de Physique Théorique et des Hautes Énergies, Université Denis Diderot, 4 place Jussieu, 75252 Paris Cedex 05, France

Received 23 December 2003 / Received in final form 6 December 2004
Published online 30 March 2005 –

Abstract. We calculate the distribution of current fluctuations in two simple exclusion models. Although these models are classical, we recover even for small systems such as a simple or a double barrier, the same distibution of current as given by traditional formalisms for quantum mesoscopic conductors. Due to their simplicity, the full counting statistics in exclusion models can be reduced to the calculation of the largest eigenvalue of a matrix, the size of which is the number of internal configurations of the system. As examples, we derive the shot noise power and higher order statistics of current fluctuations (skewness, full counting statistics, ...) of various conductors, including multiple barriers, diffusive islands between tunnel barriers and diffusive media. A special attention is dedicated to the third cumulant, which experimental measurability has been demonstrated lately.

PACS. 05.40.-a Fluctuation phenomena, random processes, noise, and Brownian motion – 73.23.-bElectronic transport in mesoscopic systems – 72.70.+m Noise processes and phenomena

1 Introduction

A constant voltage difference across a conductor drives an electrical current which will always fluctuate around its mean value. Fluctuations result from random microscopic processes (thermal relaxation, scattering, tunneling...) undergone by the charge carriers. These fluctuations can be considered as an undesirable noise but also as a rich signature of the basic transport mechanisms occurring in the conductor. This second perspective has concentrated much attention in the mesoscopic community over the last decade [1].

In our previous paper [2] we gave evidence that the statistics of current fluctuations in a large classical model, the symmetric exclusion process, are identical to the ones derived for quantum mesoscopic conductors [3]. Here, we show that exclusion models allow also to recover the current fluctuations of small systems such as a single or a double barrier.

In the present paper, we develop a classical approach to derive the statistics of current fluctuations in mesoscopic conductors ("quantum conductors") and more generally in conductors smaller than the electronic inelastic mean free path and for some inelastic conductors. Solving the current statistics problem is reduced to finding the largest eigenvalue of a modified evolution matrix, later called the *counting matrix*. We extend the well known current statistics for a few mesoscopic systems. Our description is based on the *exclusion process models*, which have been widely studied in statistical physics and probability theory [4–6]. The main benefits of this approach are its conceptual and analytical simplicity.

In the remaining part of this introduction section, we briefly recall the traditional approaches for mesoscopic transport (Sect. 1.1) and the basic mathematical tools necessary to describe current fluctuations (1.2). Section 2 presents two exclusion models fitted for condensed matter conductors and the procedure to derive the complete statistics of current fluctuations (later called "Full Counting Statistics" or FCS). In Section 3, our exclusion models are used to derive the current statistics of various elementary conductors.

1.1 Traditional formalisms for transport in condensed matter physics

A number of approaches have already been used to describe the FCS in mesoscopic conductors. The Scattering Matrix theory [3,7–13] is well adapted to the modeling of quantum-mechanically coherent conductors in a regime where electron interaction effects are sufficiently weak to be neglected. With this strong assumption, this allows to

[a] e-mail: per@grenoble.cnrs.fr

treat an arbitrary large number of transverse conduction channels, which yield independent contributions to the current statistics. This approach, combined with results from random matrix theory for scattering matrices [14] has lead to precise predictions for the FCS of a disordered conductor in the diffusive regime [15]. A more direct microscopic treatment of disordered systems relies on the Keldysh technique [16] to construct the non-equilibrium density matrix of the steady state at finite current. Disorder averaging is then performed using a non-linear Sigma model representation [17]. A rather general *circuit theory* has been constructed to account for the influence of an arbitrary environment, described in terms of an equivalent circuit, on the measured fluctuations of a mesoscopic conductor [18,19]. Semi-classical descriptions, based on the Boltzmann-Langevin model [20,21] have also been used to derive the first four cumulants of current fluctuations in a diffusive medium [22,23]. Other semi-classical approaches focused on high order statistics and FCS of a double tunnel barrier [24], chaotic cavities [25] and diffusive media [2,26]. The semi-classical results are the same as the ones obtained with the corresponding quantum conductor model.

The exclusion models discussed in this paper represent an extreme semi-classical approximation : the only quantum rule which is preserved is the Pauli exclusion principle. In particular, electrons have no phase and do not interfere.

1.2 Mathematical formalism for current fluctuations

If q_t is the algebraic charge which flows across a section during time t, the fluctuations of current $I = q_t/t$ depends in principle on the duration t chosen to measure I. In practice the long time response of the measuring electronics apparatus sets a lower bound on t: this bound is most often decades larger than all the physical times experienced by charge carriers (diffusion time, dwell time, coherence times in the conductor and in the electrodes,...). Thus, experiments correspond to the $t \to \infty$ limit, often called the zero-frequency limit in the shot noise literature. In this limit, the choice of the cross-section is irrelevant since the maximum charge accumulation between two different cross-sections is finite, at least in a conductor connected to two electrodes only.

In a conductor smaller than the inelastic mean free path, carriers do not undergo inelastic collisions. It is therefore reasonable in many situations to neglect interaction effects on such small length scales. Equivalently, we may then assume that these charge carriers remain on independent energy levels [1]. Consequently the statistics of the total current will consist in a summation of independent random variables corresponding to different energy levels. In the following, to keep equations free of elementary-charge prefactors, we focus on carriers counting rather than charge counting. In addition, we will call this generic charge carrier an *electron*.

If $P_{t,\epsilon}(Q)$ is the probability that Q electrons have been transfered at the energy level ϵ during a time interval t, one can fully characterize the counting statistics by the cumulant generating function:

$$\mathcal{S}_{t,\epsilon}(z) = \ln\left[\sum_{Q=-\infty}^{\infty} P_{t,\epsilon}(Q)\ z^Q\right] = \ln(\overline{z^Q}) \qquad (1)$$

or equivalently by cumulants (the nth order one is written here):

$$C_n(t,\epsilon) = \frac{\partial^n \mathcal{S}_{t,\epsilon}(z)}{\partial(\ln z)^n} \qquad (2)$$

we have in particular: $C_1 = \bar{Q}$, $C_2 = \overline{(Q-\bar{Q})^2}$, $C_3 = \overline{(Q-\bar{Q})^3}$, $C_4(\epsilon) = \overline{(Q-\bar{Q})^4} - 3\overline{(Q-\bar{Q})^2}^2$, ...

For a given conductor, the current at an energy level ϵ only depends on the boundary conditions, that is the fillings $\rho_{_L}(\epsilon)$ and $\rho_{_R}(\epsilon)$ of the left and right electrodes (or "reservoirs") at both ends of the conductor. If we rewrite the cumulant explicitly as $C_n(t,\epsilon,\rho_{_L},\rho_{_R})$, the cumulants $K_n(t)$ for the whole conductor are given by

$$K_n(t) = \int C_n(t,\epsilon,\rho_{_L}(\epsilon),\rho_{_R}(\epsilon))\ n(\epsilon)\ d\epsilon \qquad (3)$$

where $n(\epsilon)$ is the density of energy levels in the conductor. Likewise, the cumulant generating function for the whole conductor can be derived with the same type of summation. For comparison with experiments Fermi-Dirac distributions are imposed in the left and right electrodes:

$$\rho_{_L}(\epsilon) = \frac{1}{1+e^{\frac{\epsilon-eV}{k_BT}}}; \quad \rho_{_R}(\epsilon) = \frac{1}{1+e^{\frac{\epsilon}{k_BT}}}. \qquad (4)$$

With such fillings, the $K_n(t)$ are function of the driving voltage normalized by temperature eV/k_BT. The $k_BT \gg eV$ limit corresponds to the Johnson-Nyquist thermal noise and the opposite limit to pure shot noise. In this paper, the integration equation (3) over ϵ will be estimated assuming that $n(\epsilon)$ and $C_n(t,\epsilon,\rho_{_L},\rho_{_R})$ are independent of ϵ. This assumption is quite reasonable, since in most cases the Fermi energy in the reservoirs is much larger than both the thermal energy window k_BT and the driving energy eV.

The electrical conductance G and the current noise power density S_I are proportional to K_1 and K_2:

$$G = \overline{I}/V = eK_1/Vt; \quad S_I = 2\int \overline{\delta I(\tau)\delta I(0)}d\tau = 2e^2K_2/t \qquad (5)$$

where $\delta I(\tau) = I(\tau) - \overline{I}$ is the current fluctuation at time τ. The time scale of the model dynamics can be chosen arbitrarily since this only changes the prefactor of the cumulant generating function. The transport mechanism is characterized by the cumulants C_2, C_3,... (or K_2, K_3,...) normalized by C_1 (or K_1). In particular, we will focus on the normalized shot noise power (called the *Fano factor* in the $eV \gg kT$ limit)

$$F = S_I/2e\overline{I} = K_2/K_1 \qquad (6)$$

and the third Fano factor

$$F_3 = K_3/K_1. \qquad (7)$$

2 Exclusion models

In this section, we present two exclusion models. The first one is a classical version of the Landauer picture of a quantum conductor, where electronic wave-packets can no longer interfere (see also [26–28]). We call it the *counter-flows exclusion model* because the two directions of propagation of electrons found in a 1D conductor are explicitly considered. Conductors with a low transmission efficiency, such as tunnel barriers or diffusive media, can sometimes be described by a simpler exclusion model, presented in the *tunnel exclusion model* section. Many systems studied in the exclusion, hopping-model and sequential-tunneling literatures are directly relevant to this latter category of conductors. These models describe independent particles, apart for the exclusion constraint which represents the effect of the Pauli principle.

2.1 The counter-flows exclusion model

The counter-flows model is inspired from the Landauer [8,9,29,30] picture of conductors: at zero temperature, electrons are injected periodically from the reservoirs to the conductor. This assumption seems a good enough modeling to account for the FCS in the $t \to \infty$ limit. Indeed, the predictions of the model would remain unchanged if the variance $\overline{(N_t - \overline{N_t})^2}$ of the number of injection attempts N_t during a time interval t, is only sublinear in t. This later property follows from the Pauli exclusion in degenerate electrodes which imposes an anti-correlation between injection events [3,12]. The experimental validation of Landauer approach [1,31,32] justifies a posteriori this nearly-periodic injection model. While in the sample, these charge carriers may undergo internal scattering on localized barriers and finally are either reflected or transmitted to electrodes at both ends of the conductors. The Pauli exclusion principle is fulfilled at each stage during the system evolution.

More precisely, the $2N$ sites counter-flows model consists in $N+1$ barriers, each characterized by 2 transmission probabilities $\Gamma_i^{(\rightarrow)}$ (from left to right) and $\Gamma_i^{(\leftarrow)}$ (from right to left) where i is the index of the barrier increasing from left to right ($1 \leq i \leq N+1$). Between two consecutive barriers, 2 sites are available for at most 2 electrons propagating in opposite directions. So a configuration at time t is characterized by $2N$ binary variables $\tau_i^{(\rightarrow)}(t)$ and $\tau_i^{(\leftarrow)}(t)$ for $1 \leq i \leq N$; $\tau_i^{(\rightarrow)}(t)$ (respectively $\tau_i^{(\leftarrow)}(t)$) is equal to 1 if an electron propagating to the right (respectively to the left) is present at site i at time t. Time is discrete and at each time step, electrons are transmitted through one barrier to the next site, unless a back-scattering occurs on the barrier. By definition of the dynamics of the model, $\tau_{i+1}^{(\rightarrow)}(t+1)$ and $\tau_i^{(\leftarrow)}(t+1)$ depend only on $\tau_i^{(\rightarrow)}(t)$ and on $\tau_{i+1}^{(\leftarrow)}(t)$, and the (classical) transition probabilities are given in Figure 1. This allows for a simultaneous update of all occupancies, even in the presence of backscattering on barriers.

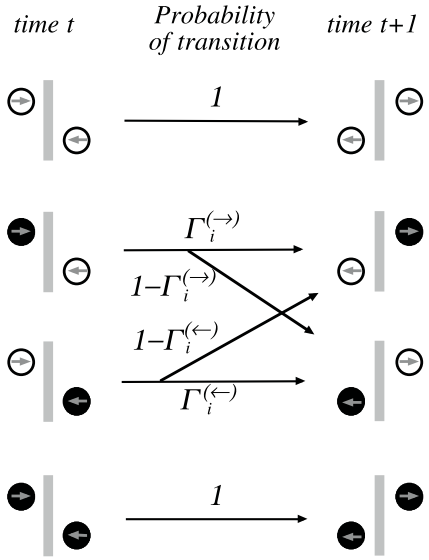

Fig. 1. Counter-flows model. Probability of evolution for the various configurations of electrons reaching the ith barrier at time t.

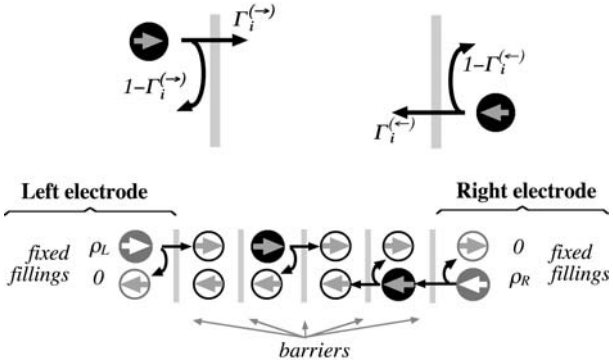

Fig. 2. Counter-flows model. Upper figure: Transmission and reflection probabilities for the ith barrier, assuming no conflict with the exclusion principle. Lower figure: The counter-flows model for $N = 4$. The white circles represent empty sites, the black disks are electrons, the gray disks stand for sites with a fixed filling probability and the arrows indicate the direction of propagation associated with each site.

At the boundaries of the conductors, each electrode is modeled by 2 sites, the occupation states of which are re-set before each time step. The site corresponding to an electron propagating into the conductor is re-filled with probability ρ_L (left electrode) or ρ_R (right electrode) and the site accessible to the electron leaving the conductor is re-emptied at each time step (see Fig. 2). The densities ρ_L and ρ_R are given by Fermi-Dirac distributions (Eq. (4)). After this reset, the one-time-step evolution follows the same transmission/back-scattering rule that holds in the bulk of the conductor.

On modeling real conductors, the barriers can represent junctions (between two different materials for example), scattering centers (impurities, structural defects, ...) or even inelastic processes (phonon or photon-assisted hopping, emission of phonon or photon, ...). The model

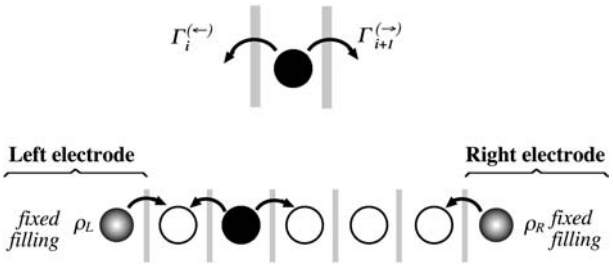

Fig. 3. Tunnel model. Upper figure: Tunneling probabilities across the ith and $(i+1)$th barriers for an electron located between them, assuming no conflict with the exclusion principle. Lower figure: Tunnel exclusion model for $N = 5$ sites.

parameters N, $\Gamma_i^{(\leftarrow)}$ and $\Gamma_i^{(\rightarrow)}$ are related to the corresponding physical quantities such as tunneling probabilities or scattering cross-sections.

2.2 The tunnel exclusion model

It is useful to note that the counter-flows exclusion model may be decomposed into two independent stochastic models. Let us define new variables $\sigma_i(t)$ and $\sigma'_i(t)$ such that $\sigma_i(t) = \tau_i^{(\rightarrow)}(t)$ if i and t have the same parity and else $\sigma_i(t) = \tau_i^{(\leftarrow)}(t)$. In a similar way, $\sigma'_i(t) = \tau_i^{(\leftarrow)}(t)$ if i and t have the same parity and else $\sigma'_i(t) = \tau_i^{(\rightarrow)}(t)$. From the definition of the model, the random variables σ_i are completely decoupled from the σ'_i variables. It turns out that in the limit of small transmission probabilities, the dynamics of each of these two ensembles of binary variables may be formulated in terms of a simpler lattice model, that we shall call the *tunnel exclusion model*. The elementary time-step of the latter model involves two steps in the former one. This has the advantage that in the limit of a vanishing transmission probability, the configuration of σ_i's does not evolve in time. For each of these two independent submodels, expanding the evolution of this reduced system to first order in transmission probabilities, and taking the continuous time limit, we get the model which definition is sketched on Figure 3. In this case, the quantities $\Gamma_i^{(\rightarrow)}$ and $\Gamma_i^{(\leftarrow)}$ become the probabilities per time unit of tunneling across the ith barrier from left to right and vice-versa, provided that the target site is empty. Each electrode is modeled by a single site, the occupation of which is reset to ρ_L (left electrode) or ρ_R (right electrode) before each time step. The fillings ρ_L and ρ_R are given by Fermi-Dirac distributions (See Eq. (4).)

A special choice of the tunneling probabilities is the *Symmetric Simple Exclusion Process* or SSEP [33] (see Fig. 4) for which the the internal barriers are symmetric ($\Gamma_i^{(\leftarrow)} = \Gamma_i^{(\rightarrow)}$) and uniform along the conductor (independent of i for $2 \leq i \leq N$). We note this probability Γ. The two out-most barriers are also modeled with symmetric rates $\Gamma_L = \Gamma_1$ and $\Gamma_R = \Gamma_{N+1}$. Physically they account for the electrical connection between the electrodes and the conductor. In the theory of exclusion processes [2], one usually represents the reservoirs by injection rates α, δ, and extraction rates γ, β which give

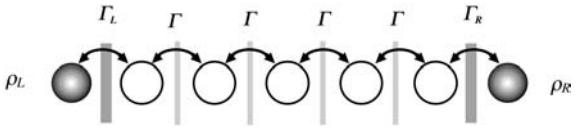

Fig. 4. SSEP model for $N = 5$ sites. Γ_L, Γ and Γ_R are the tunneling probabilities and ρ_L, ρ_R the electrodes' fixed fillings.

an equivalent description of the boundary conditions if: $\alpha = \rho_L\Gamma_L, \delta = \rho_R\Gamma_R, \gamma = (1-\rho_L)\Gamma_L, \beta = (1-\rho_R)\Gamma_R$.

2.3 The FCS solving procedure

In the counter-flows model, the conductor has 2^{2N} internal configurations $\mathcal{C} = \left\{\tau_1^{(\rightarrow)}, \tau_1^{(\leftarrow)}, ..., \tau_N^{(\rightarrow)}, \tau_N^{(\leftarrow)}\right\}$. Let $p_t(\mathcal{C})$ be the probability of finding the system in configuration $\mathcal{C}$ at time t. As the dynamics is a Markov process, the evolution equation for $p_t(\mathcal{C})$ can be written:

$$p_{t+1}(\mathcal{C}) = \sum_{\mathcal{C}'}[M_1(\mathcal{C},\mathcal{C}') + M_0(\mathcal{C},\mathcal{C}') + M_{-1}(\mathcal{C},\mathcal{C}')]p_t(\mathcal{C}') \tag{8}$$

where we have decomposed the evolution matrix into three parts M_1, M_0 and M_{-1}, depending on whether, when the system jumps from configuration $\mathcal{C}'$ to configuration $\mathcal{C}$, the total number of charges transfered from the system to the right reservoir increases by $1, 0$ or -1.

If we define $P_t(\mathcal{C}, Q)$ as the probability that the system is in configuration $\mathcal{C}$ at time t and that Q charges have been transfered, one has:

$$P_{t+1}(\mathcal{C},Q) = \sum_{\mathcal{C}'} M_1(\mathcal{C},\mathcal{C}')P_t(\mathcal{C}',Q-1) + M_0(\mathcal{C},\mathcal{C}')P_t(\mathcal{C}',Q) + M_{-1}(\mathcal{C},\mathcal{C}')P_t(\mathcal{C}',Q+1). \tag{9}$$

Then the generating functions $\mathcal{P}_t(\mathcal{C}, z)$ defined by:

$$\mathcal{P}_t(\mathcal{C},z) = \sum_{Q=-\infty}^{\infty} P_t(\mathcal{C},Q)\ z^Q \tag{10}$$

satisfies

$$\mathcal{P}_{t+1}(\mathcal{C},z) = \sum_{\mathcal{C}'}\left[z\ M_1(\mathcal{C},\mathcal{C}') + M_0(\mathcal{C},\mathcal{C}') + \frac{1}{z}M_{-1}(\mathcal{C},\mathcal{C}')\right]\mathcal{P}_t(\mathcal{C}',z). \tag{11}$$

If we introduce M_z that we will call the *counting matrix*, defined by:

$$M_z(\mathcal{C},\mathcal{C}') = z\ M_1(\mathcal{C},\mathcal{C}') + M_0(\mathcal{C},\mathcal{C}') + \frac{1}{z}M_{-1}(\mathcal{C},\mathcal{C}') \tag{12}$$

it is clear from equation (11) that in the long time limit, the cumulant generating function for the total number of transfered charges is:

$$\mathcal{S}_t(z) = \ln(\overline{z^Q}) = \ln\left[\sum_{\mathcal{C}}\mathcal{P}_t(\mathcal{C},z)\right] \sim \ln\left(\nu(z)^t\right) \sim t\ln\left(\nu(z)\right) \tag{13}$$

Table 1. Asymmetric Single Barrier for arbitrary fillings $\rho_{_L}$ and $\rho_{_R}$ of the electrodes. The full circles represent occupied sites.

evolution	charge counting	probability
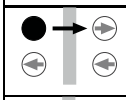	increase	$\rho_{_L}(1-\rho_{_R})\Gamma^{(\rightarrow)}$
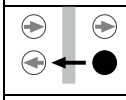	decrease	$(1-\rho_{_L})\rho_{_R}\Gamma^{(\leftarrow)}$
others	unchanged	$1-\rho_{_L}(1-\rho_{_R})\Gamma^{(\rightarrow)}-(1-\rho_{_L})\rho_{_R}\Gamma^{(\leftarrow)}$

where $\nu(z)$ is the largest eigenvalue of the counting matrix M_z [2,34]. Due to the fact (see beginning of Sect. 2.2) that the counter-flows model can be decomposed into two decoupled sets of variables, the eigenvalue $\nu(z)$ can in fact be obtained by diagonalizing a $2^N \times 2^N$ matrix.

In the tunnel exclusion model, the conductor has 2^N internal configurations and – as previously – we call $p_t(\mathcal{C})$ the probability of finding the system in configuration $\mathcal{C}$ at time t. The time being continuous in this model, one has:

$$\frac{dp_t(\mathcal{C})}{dt} = \sum_{\mathcal{C}'} \left[W_1(\mathcal{C},\mathcal{C}') + W_0(\mathcal{C},\mathcal{C}') + W_{-1}(\mathcal{C},\mathcal{C}')\right] p_t(\mathcal{C}') \tag{14}$$

where the evolution matrix has been decomposed into three parts W_1, W_0 and W_{-1}, depending on whether when the system jumps from configuration $\mathcal{C}'$ to configuration $\mathcal{C}$, the total number of transfered charges increases by $1, 0$ or -1. Equation (14) is a continuous time version of equation (9), the main difference being the diagonal elements of W_0 are now all negative.

Following the same procedure as above, we can define the *counting matrix* W_z by:

$$W_z(\mathcal{C},\mathcal{C}') = z\; W_1(\mathcal{C},\mathcal{C}') + W_0(\mathcal{C},\mathcal{C}') + \frac{1}{z} W_{-1}(\mathcal{C},\mathcal{C}') \tag{15}$$

and we find the cumulant generating function for the total transfered charge in the long time limit:

$$\mathcal{S}_t(z) = \ln(\overline{z^Q}) \sim \ln\left(e^{\mu(z)\;t}\right) \sim t\;\mu(z) \tag{16}$$

where $\mu(z)$ is the largest eigenvalue of the counting matrix W_z. This latter equation can be seen as the first term in the expansion of the corresponding equation obtained in a discrete time approach in the limit of small transmission.

Both for the counter-flows and tunnel models, the FCS is fully determined by the largest eigenvalue of what we called the *counting matrix*.

The full knowledge of the eigenvalue is not necessary if only the first n cumulants are wanted. In this case, the equation satisfied by the eigenvalues $|M_z - \nu(z)\mathcal{I}| = 0$ (or $|W_z - \mu(z)\mathcal{I}| = 0$) can be solved by a perturbation theory and the nth cumulant is obtained from the coefficient of the nth order of the eigenvalue in powers of $\log(z)$ (see Eq. (2)). Once the counting matrix is written down, this procedure can be easily performed by an analytical calculation software.

3 Application to mesoscopic systems

In the remaining of this paper we derive the FCS or the first cumulants of basic mesoscopic systems. A special attention is dedicated to the current fluctuations skewness (third cumulant) and its associated third Fano factor, the physical interest ([35,36]) and measurability [37] of which have been recently emphasized. Indeed, at high temperature the skewness can reveal information about transport which are not blurred by thermal fluctuations [35,36]. Some of the results derived are already known and they validate exclusion modeling for charge conduction in condensed-matter systems. The various new results, often derived in a few lines of linear algebra, illustrate the strength of this modeling.

3.1 Asymmetric barrier and single channel

The counter-flows model with $N = 0$ site is a single barrier between two electrodes of fillings $\rho_{_L}$ and $\rho_{_R}$. Since the system has no internal state, the counting matrix M_z is a scalar. A positive charge transfer (from left to right) will occur with probability $p_+ = \rho_{_L}(1-\rho_{_R})\Gamma^{(\rightarrow)}$ and a negative transfer with probability $p_- = (1-\rho_{_L})\rho_{_R}\Gamma^{(\leftarrow)}$ (see Tab. 1).

Following the general procedure for the counter-flows model, we consider the counting "matrix":

$$M_z = p_+\; z \;+\; p_-\; z^{-1} + (1 - p_+ - p_-). \tag{17}$$

The logarithm of the largest (and unique) eigenvalue $\nu(z) = M_z$ gives the cumulant generating function $\mathcal{S}_t(z)$, which fully characterize the FCS of an asymmetrical barrier:

$$\mathcal{S}_t(z)/t = \ln\Big\{ \left[\rho_{_L}\;(1-\rho_{_R})\;\Gamma^{(\rightarrow)}\right]\;(z-1) + \left[(1-\rho_{_L})\;\rho_{_R}\,\Gamma^{(\leftarrow)}\right]\;\left(z^{-1}-1\right)\;+1\Big\} \tag{18}$$

A few particular cases are interesting:

- The $\Gamma^{(\rightarrow)}, \Gamma^{(\leftarrow)} \rightarrow 1$ limits account for quasi-ballistic barriers. On the opposite case of tunnel barriers ($\Gamma^{(\rightarrow)}, \Gamma^{(\leftarrow)} \ll 1$), the FCS can be re-estimated from a first order expansion of equation (18) or directly with the

tunnel exclusion model with $N = 0$:

$$\mathcal{S}_t(z)/t = \mu(z) = W_z = \rho_{_L}(1-\rho_{_R})\Gamma^{(\rightarrow)}(z-1) + (1-\rho_{_L})\rho_{_R}\Gamma^{(\leftarrow)}(z^{-1}-1) \quad (19)$$

• The asymmetric case ($\Gamma^{(\rightarrow)} \neq \Gamma^{(\leftarrow)}$) accounts for inelastic barrier, such as those for which stepping over the barrier requires the emission or assistance of a photon or phonon [35].

For symmetric barriers

$$\mathcal{T} = \Gamma^{(\rightarrow)} = \Gamma^{(\leftarrow)} \quad (20)$$

we recover the important case of a *conduction channel* of transparency $\mathcal{T}$ encountered in mesoscopic transport [12]. Once the behavior of a single conduction channel has been determined, scattering matrix theory shows how to reduce the problem of interaction-less electronic transport through a quantum constriction into a set of independent symmetric barriers. In the zero temperature limit, the only states which contribute to the FCS are those whose energy ϵ is such that $\rho_{_L}(\epsilon) = 1$ and $\rho_{_R}(\epsilon) = 0$, or $\rho_{_L}(\epsilon) = 0$ and $\rho_{_R}(\epsilon) = 1$. The FCS is then given as a superposition of independent binomial laws ("partition noise"), one for each of these scattering states, lying in an energy window eV, where V is the voltage drop across the barrier [12]. In the high temperature limit, one has to integrate the single channel result equation (18) over the complete Fermi-Dirac distributions in the reservoirs, given in equation (4).

From equations (2), (3), (18) and ($\mathcal{T} = \Gamma^{(\rightarrow)} = \Gamma^{(\leftarrow)}$), one can derive the normalized noise power $F = K_2/K_1$ in the low temperature limit (Fano factor) and the third Fano factor $F_3 = K_3/K_1$ in the high temperature limit [17,35]. It is interesting to note that these two quantities turn out to be equal. More generally, for a mesoscopic conductor decomposed into independent channels of transparencies $\mathcal{T}_i$ one has:

$$F(eV \gg k_BT) = F_3(eV \ll k_BT) = \frac{\sum \mathcal{T}_i(1-\mathcal{T}_i)}{\sum \mathcal{T}_i}. \quad (21)$$

The physical information contained in the third cumulant at high temperature [35,36] is the same at the one contained in the low temperature second cumulant.

The first equality in equation (21) will be directly checked for the semi-classical mesoscopic systems considered in the rest of this paper.

3.2 Double barriers

For single barriers, the agreement between the exclusion model and mesoscopic models is not surprising since the boundary conditions (injection from the electrodes,...) are identical. The next step is to assess the validity of exclusion models for double barriers, for which it is crucial to account properly for both the boundary conditions and the Pauli exclusion principle inside the conductor.

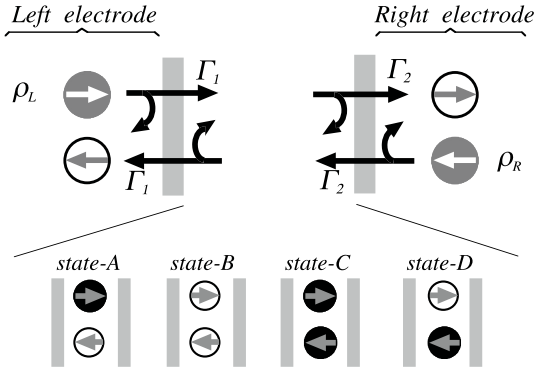

Fig. 5. Upper figure: Double symmetrical barriers (counter-flows model with $N = 1$, $= \Gamma_i^{(\rightarrow)} = \Gamma_i$). For legibility, the reflection probabilities $1-\Gamma_1$ and $1-\Gamma_2$ are not written. Lower figure: The internal states of the system.

Double barriers have been widely studied because a rich behavior results from the interplay of various effects including Pauli exclusion principle, Coulomb interactions, inelastic processes and quantum resonance [1]. In this section, we do our calculation on a generic double barrier. Then we see how this system relates to various experimental devices (quantum dots, hopping on localized states, islands and wells) and how the Coulomb interaction between electrons can be introduced to account for charging effects. The case of a partly or fully diffusive island between two tunnel barriers is addressed in Section 3.3.

Generic double barrier

We first consider two symmetric barriers of transmission Γ_1 and Γ_2, temporarily in the zero temperature limit $eV \gg k_BT$ ($\rho_{_L} = 1$ and $\rho_{_R} = 0$). The upper graph of Figure 5 depicts the corresponding counter-flows model, with $N = 1$, while the lower graph labels the 2^{2N} internal states of the system.

If the charge counting is done over the second barrier (arbitrary choice), the counting matrix M_z is:

$$M_z = \begin{pmatrix} \Gamma_1\Gamma_2 z & \Gamma_1 & \Gamma_2 z & 1 \\ (1-\Gamma_1)\Gamma_2 z & 1-\Gamma_1 & 0 & 0 \\ \Gamma_1(1-\Gamma_2) & 0 & 1-\Gamma_2 & 0 \\ (1-\Gamma_1)(1-\Gamma_2) & 0 & 0 & 0 \end{pmatrix}. \quad (22)$$

In this matrix, the states are ordered from state-A (upper-left) to state-D (lower-right). The eigenvalues of M_z can be easily found and the cumulant generating function $\mathcal{S}_t(z)$ is proportional to the logarithm of the largest one:

$$\mathcal{S}_t(z)/t = \ln\left(1 - \frac{\Gamma_1+\Gamma_2-\Gamma_1\Gamma_2 z}{2} + \sqrt{\left(1-\frac{\Gamma_1+\Gamma_2-\Gamma_1\Gamma_2 z}{2}\right)^2 - (1-\Gamma_1)(1-\Gamma_2)}\right). \quad (23)$$

The symmetry of this expression between Γ_1 and Γ_2 illustrates that the charge counting can be performed on

$$C_2/t = \frac{\Gamma_1\Gamma_2\Gamma_{12}^2(\rho_L+\rho_R) - (\rho_L^2+\rho_R^2)\Gamma_1^2\Gamma_2^2(2-\Gamma_{12}) - 2\rho_L\rho_R\Gamma_1\Gamma_2(\Gamma_1^2+\Gamma_2^2-\Gamma_1\Gamma_2(\Gamma_1+\Gamma_2))}{\Gamma_{12}^3}. \quad (26)$$

$$F_3(eV \gg k_BT) = \frac{\Gamma_1^4+\Gamma_2^4+\Gamma_1^3\Gamma_2^3(4+\Gamma_1+\Gamma_2)+\Gamma_1^2\Gamma_2^2(6-3\Gamma_1-\Gamma_1^2-3\Gamma_2-\Gamma_2^2)-\Gamma_1\Gamma_2(2\Gamma_1^2+\Gamma_1^3+2\Gamma_2^2+\Gamma_2^3)}{\Gamma_{12}^4} \quad (27)$$

any side of the system without changing the result. As expected, the single barrier FCS is recovered if one barrier is transparent (Γ_1 or $\Gamma_2 = 1$). Equation (23) extends two other results first obtained by de Jong in the Boltzmann-Langevin formalism: the first and second cumulants of a double barrier [27] and the FCS of a double tunnel barrier ($\Gamma_1\Gamma_2 \ll 1$) [24]. It is interesting to relate the classical expression equation (23) with the one derived by a full quantum treatment of the double barrier system. As described below, such a precise connection may be established in the tunneling regime where both transmissions Γ_1 and Γ_2 are very small. A generalization for arbitrary transmissions is presented in the appendix.

For arbitrary fillings ρ_L and ρ_R of the electrodes, the counting matrix M_z has no zero element and the eigenvalue problem is still manageable but more tedious. Considering instead the 2×2 counting matrix associated with one of the two independent submodels (see beginning of Sect. 2.2) makes the eigenvalue problem straightforward again. The power expansion method presented in Section 2.3 is chosen here to derive the cumulants C_1, C_2 and C_3, and integration over Fermi-Dirac distribution in the electrodes, according to equations (3) and (4), gives the cumulants $K_1(eV/k_BT)$, $K_2(eV/k_BT)$ and $K_3(eV/k_BT)$. It is useful to define:

$$\Gamma_{12} = \Gamma_1 + \Gamma_2 - \Gamma_1\Gamma_2. \quad (24)$$

One finds

$$C_1/t = (\rho_L - \rho_R)\frac{\Gamma_1\Gamma_2}{\Gamma_{12}} \quad (25)$$

see equation (26) above

For $eV \ll k_BT$, we find $K_2/K_1 = 2k_BT/eV$, that is the well known Johnson-Nyquist thermal noise formula, more often written $S_I = 4k_BTG$ where the conductance G and the current noise power spectral density S_I are given by equation (5).

We focus now on the third Fano factor $F_3 = K_3/K_1$. We give below its $eV \gg k_BT$ and $eV \ll k_BT$ limits, which -as would be expected from a quantum mechanical derivation (Eq. (21)) – is equal to the normalized noise power $F = K_2/K_1$ in the zero temperature limit (Fano factor). Figure 6 shows that depending of Γ_1 and Γ_2, the third Fano factor changes sign in the low temperature limit (left Fig. 6) and not in the high temperature one (right Fig. 6). The insert on the left figure shows $F_3 = (1-\Gamma_1\Gamma_2/\Gamma_{12})(1-2\Gamma_1\Gamma_2/\Gamma_{12})$ obtained when the exclusion principle is deactivated between the two barriers. The change of sign is still observed and thus, it cannot be attributed to correlation inducted by the exclusion principle inside the conductor.

see equation (27) above

$$F_3(eV \ll k_BT) = 1 - \frac{\Gamma_1\Gamma_2(2-\Gamma_{12})}{\Gamma_{12}^2} = F(eV \gg k_BT). \quad (28)$$

Tunnel limit

The FCS of a double tunnel barrier can be obtained from the general expression equation (23) for the double barrier. Nevertheless, it is interesting to derive it with the Symmetric Simple Exclusion Model with $N = 1$. For arbitrary fillings ρ_L and ρ_R of the electrodes, and charge counting done over the second barrier, the counting matrix is:

$$W_z = \begin{pmatrix} -\Gamma_2(1-\rho_R) - \Gamma_1(1-\rho_L) & \Gamma_1\rho_L + \Gamma_2\rho_R z^{-1} \\ \Gamma_2(1-\rho_R)z + \Gamma_1(1-\rho_L) & -\Gamma_1\rho_L - \Gamma_2\rho_R \end{pmatrix}. \quad (29)$$

Following Section 2.3, the cumulant generating function $\mathcal{S}_t(z)$ is proportional to the largest eigenvalue of W_z. After a few lines of algebra, we find:

$$\mathcal{S}_t(z)/t = -\frac{\Gamma_1+\Gamma_2}{2} + \left(\left(\frac{\Gamma_1+\Gamma_2}{2}\right)^2 + \Gamma_1\Gamma_2\Big(\rho_L(1-\rho_R)(z-1) + \rho_R(1-\rho_L)(z^{-1}-1)\Big)\right)^{1/2}. \quad (30)$$

We recover the FCS derived in [38], which slightly differs from the one derived in [39].

Experimental systems

Depending on the elastic or inelastic nature of the barriers, several double barrier systems are traditionally considered. If we restrict ourselves to elastic barriers, the size of the island between the barriers is another source of experimental diversity.

In large but finite-size islands ("quantum island"), the quasi energy levels are discrete and the generic system described above can model each such level. At this stage, it may be useful to describe in more detail the connection between a microscopic quantum coherent model for a single conducting channel in the presence of a double barrier

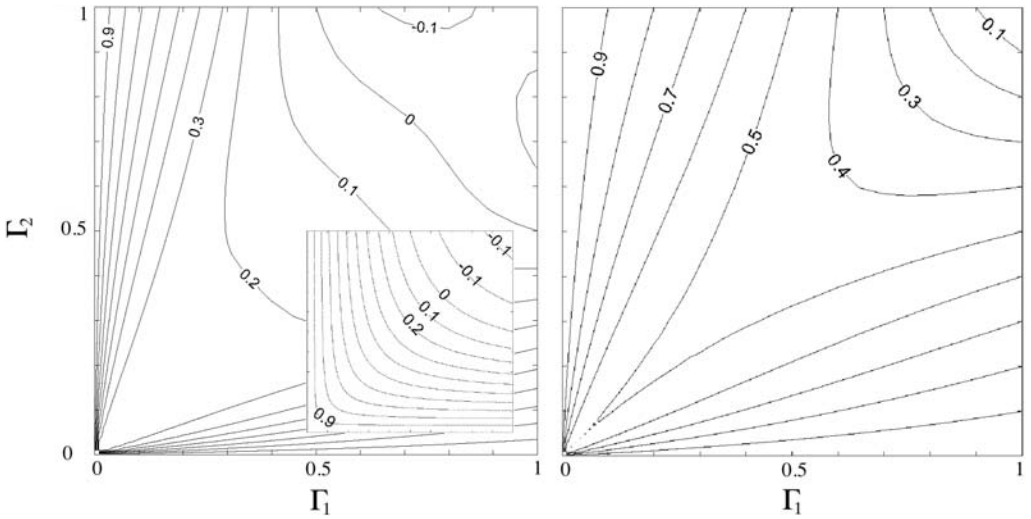

Fig. 6. Third Fano factor $F_3 = K_3/K_1$ for a double symmetrical barrier. Left figure: Zero temperature limit ($eV \gg k_BT$) (insert: the exclusion principle is deactivated between the barriers). Right figure: High temperature limit ($k_BT \gg eV$).

in the tunneling limit, and the corresponding SSEP. At zero temperature, the generating function $\mathcal{S}_t(z)/t$ for the microscopic quantum model is given by [12]:

$$\mathcal{S}_t(z)/t = v_F \int_{k_{\min}}^{k_{\max}} \frac{dk}{2\pi} \ln(\mathcal{T}(k)(z-1)+1),$$

where $\mathcal{T}(k)$ is the transmission coefficient for an incoming electronic wave-function with wave-vector k and $k_{\max} - k_{\min} = \frac{eV}{\hbar v_F}$, v_F being the Fermi velocity in the electrodes. For a fully coherent system, $\mathcal{T}(k)$ has to obey the quantum series composition rule for transmission matrices. In the limit of small transmissions $\mathcal{T}_1$ and $\mathcal{T}_2$, this yields the well-known Lorentzian resonance profile:

$$\mathcal{T}(k) = \frac{4\mathcal{T}_1\mathcal{T}_2}{(\mathcal{T}_1+\mathcal{T}_2)^2 + 16(k-k_0)^2 l^2},$$

where l is the distance between the two barriers. In the limit where $eV/\hbar$ is much larger than the decay rate $\gamma = \frac{v_F}{2l}(\mathcal{T}_1+\mathcal{T}_2)$ of the resonant level in the central region, and if the average energy of this level is such that k_0 falls in the interval $[k_{\min}, k_{\max}]$, we may take the k integration over the whole real axis, yielding exactly equation (30) in the special case $\rho_{_L}(\epsilon) = 1$ and $\rho_{_R}(\epsilon) = 0$, provided we set $\Gamma_i = \frac{v_F}{2l}\mathcal{T}_i$ $(i = 1, 2)$ [24]. So in the tunnel limit, the simple SSEP may be viewed as the result of integrating the contributions of quantum-mechanically coherent electrons over an energy window larger than the width $\hbar\gamma$ of a discrete level inside the cavity delimited by the two barriers.

When the island is infinite in the transverse direction ("Quantum well"), the energy levels become a continuous energy band: the generic model still applies but the integration equation (3) should be done versus wavevectors [1] $k_\parallel$ (longitudinal) and $k_\perp$ (transverse direction) rather than versus the energy ϵ.

Finally, when the island is small ("Quantum dot") or when it consists in localized states (dopants, impurities...),

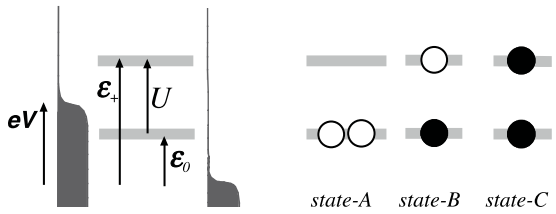

Fig. 7. Left figure: Energy levels associated with the two sites in interaction. Right figure: The three internal states of the system. Each black disk represents an electron and each circle represents an available site with spin degeneracy.

the energy levels are well separated but one can no longer neglect that electrons entering or leaving the island are changing its Coulomb electrostatic energy, which induces a shift of the energy levels ("charging effect"). We illustrate in the simple example below how to account for such an effect.

Charging effect

We consider now two localized states tunnel-coupled to two electrodes with Fermi-Dirac fillings $\rho_{_L}(\epsilon)$ and $\rho_{_R}(\epsilon)$ (Fig. 7). The coupling is elastic (for example, it could be due to some overlapping of the localized state wavefunction with electrodes) and characterized by two symmetrical transmission coefficients $\Gamma_1, \Gamma_2 \ll 1$. So we assume that an electron can be transfered from one electrode to the other by a sequential tunneling process through one of the two localized states. Because of large on-site Coulomb interaction, at most one electron, with spin up or down, can be trapped on each localized state. To model intersite charging effects, we assume that the localized sites contribution to the energy is $E_{\rm loc}(n_1, n_2) = \epsilon_1 n_1 + \epsilon_2 n_2 + U n_1 n_2$ where n_1 and n_2 are the occupation numbers, ϵ_1 and ϵ_2 are the single level energies and $U > 0$ is an electrostatic energy. Such a model has already been proposed [40] to explain experimental data. Our purpose in this section is

$$W_z = \Gamma \begin{pmatrix} -4\rho_L(\epsilon_0) - 4\rho_R(\epsilon_0) & (1-\rho_L(\epsilon_0)) + (1-\rho_R(\epsilon_0))z & 0 \\ 4\rho_L(\epsilon_0) + 4\rho_R(\epsilon_0)/z & -2 + \rho_L(\epsilon_0) - 2\rho_L(\epsilon_+) + \rho_R(\epsilon_0) - 2\rho_R(\epsilon_+) & 2(1-\rho_L(\epsilon_+)) + 2(1-\rho_R(\epsilon_+))z \\ 0 & 2\rho_L(\epsilon_+) + 2\rho_R(\epsilon_+)/z & -4 + 2\rho_L(\epsilon_+) + 2\rho_R(\epsilon_+)) \end{pmatrix} \quad (31)$$

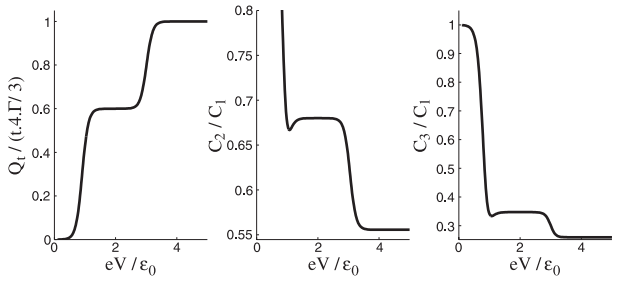

Fig. 8. Two sites interacting via the Coulomb electrostatic repulsion and tunnel coupled to electrodes (see text). Left figure: Normalized current $C_1/(t4\Gamma/3)$. Central figure: Normalized noise power C_2/C_1. Right figure: Third Fano factor C_3/C_1.

to illustrate how exclusion models can deal with charging effect. For the sake of clarity, we therefore restricted ourselves to degenerated energy levels $\epsilon_0 = \epsilon_1 = \epsilon_2$ and $\Gamma = \Gamma_1 = \Gamma_2$. This system has three internal states, corresponding to 0, 1 or 2 trapped electrons (States A, B and C in Fig. 7) and the corresponding counting matrix is

see equation (31) above

where $\epsilon_+ = \epsilon_0 + U$. With a software like Mathematica, the analytical equations for the cumulants C_1, C_2 and C_3 are easily derived by the series expansion method (Sect. 2.3). These expressions are not reported here but have been used to generate the normalized cumulants of Figure 8 for parameters $\epsilon_0/k_BT = 10$, $U/k_BT = 20$ and $\Gamma \ll 1$. The first cumulant C_1 is normalized by the averaged transfer charge $4.t.\Gamma/3$ expected in the high driving voltage limit.

Similar stochastic classical models have also been studied to account for transport through quantum dot above the Kondo temperature (see for example [38,41,42]). Below this temperature, classical models are no longer expected to be meaningful.

3.3 Multiple barriers: from double wells to diffusive islands between tunnel contacts

In this section we discuss the general SSEP model presented at the end of Section 2.2 , $(N-1)$ identical barriers of transmission $\Gamma \ll 1$ are sandwiched between two tunnel barriers of transmission Γ_L and Γ_R. Although a single chain of sites is considered, this situation is expected to account for physical systems with a large number of transverse conduction channels. This is justified a-posteriori by the perfect quantitative agreement between the predictions of the classical models and the full quantum mechanical derivation for multi-channels systems (see below).

Writing down that the mean current and its variance do not depend on the barrier over which they are measured, we showed in [2] how to derive the first two cumulants:

$$C_1/t = \frac{\Gamma}{N_1}(\rho_L - \rho_R) \quad (32)$$

$$C_2/t = \frac{\Gamma}{N_1}\left[(\rho_L + \rho_R - 2\rho_L\rho_R) - \frac{2}{3}(\rho_L - \rho_R)^2\left(1 - \frac{1}{2N_1} - \frac{\lambda}{2{N_1}^2(N_1-1)}\right)\right] \quad (33)$$

with $N_1 = N - 1 + \frac{\Gamma}{\Gamma_L} + \frac{\Gamma}{\Gamma_R}$ and $\lambda = \frac{\Gamma}{\Gamma_L}\left(\frac{\Gamma}{\Gamma_L} - 1\right)\left(2\frac{\Gamma}{\Gamma_L} - 1\right) + \frac{\Gamma}{\Gamma_R}\left(\frac{\Gamma}{\Gamma_R} - 1\right)\left(2\frac{\Gamma}{\Gamma_R} - 1\right)$

For arbitrary N_1, the third cumulant C_3 can be derived from the third order series expansion of the cumulant generating function given in [2] (Eq. (C.14)). We give below the third Fano factor in the large N_1 (or N) limit.

Experimental systems

Three limiting cases of the above general formula could be relevant to mesophysics.

- Firstly, for $N = 2$, the system is a triple barrier with three different tunnel transmissions. Such systems have been widely studied as a model for double localized state, coupled quantum dot and double well structures (for example see [1,43]). It would be interesting to compare our predictions to the experimental results.
- In the limit $N \to \infty$ for constant Γ, Γ_L and Γ_R, the relative contribution of the two out-most barriers is vanishingly small and we obtain a diffusive medium in good contact with the electrodes. Section 3.4 addresses this purely diffusive regime and gives its FCS. At this point, we just point that C_1 and C_2 are in agreement with the one found by alternative condensed-matter formalisms [22,27,44–48]. It is specially interesting to note that a one dimensional classical stochastic model is able to reproduce current fluctuations arising in a 3 dimensional coherent diffusive conductor.
- The limit $N \to \infty$ for constant Γ, $N\Gamma_L$ and $N\Gamma_R$ accounts for a diffusive island between two tunnel contacts, the resistances of which are comparable to the resistance of the diffusive island itself. We define as $q_L = \Gamma/(N\Gamma_L)$ and $q_R = \Gamma/(N\Gamma_R)$ the ratios of the left and right contact resistances over the diffusive island resistance. The large q_L and q_R limit accounts for simple or double tunnel barriers while vanishing values of q_L and q_R account for a purely diffusive medium.

The normalized noise power F (Eq. (6)), is found to be, for an arbitrary temperature:

$$F = \frac{K_2}{K_1} = \frac{2k_BT}{eV}(1-s) + s\coth\left(\frac{eV}{2k_BT}\right) \quad (34)$$

Table 2. First cumulants C_n for diffusive medium for arbitrary filling of the electrodes, and low and high temperature normalized cumulants K_n/K_1. ($X = (\rho_L - \rho_R)$ and $Y = (\rho_L + \rho_R - 1)$).

n	*Normalized cumulants:* $\frac{C_n}{(t\Gamma/N)}$	K_n/K_1 for $k_BT \ll eV$	K_n/K_1 *for* $k_BT \gg eV$
1	X	1	1
2	$\left[3 - X^2 - 3Y^2\right]/6$	$\frac{1}{3}$	$\frac{2k_BT}{eV}$
3	$X^3/15 + XY^2$	$\frac{1}{15}$	$\frac{1}{3}$
4	$\left[-9X^4 + X^2\left(7 - 462Y^2\right) - 105Y^2\left(-1 + Y^2\right)\right]/210$	$-\frac{1}{105}$	$\frac{2k_BT}{3eV}$
5	$4X^5/105 + XY^2\left(-3 + 4Y^2\right) + X^3\left(-1 + 120Y^2\right)/21$	$-\frac{1}{105}$	$-\frac{1}{5}$
6	$[-20X^6 - 33X^4\left(-1 + 244Y^2\right) - 231Y^2\left(3 - 7Y^2 + 4Y^4\right) - 11X^2\left(1 - 618Y^2 + 1044Y^4\right)]/462$	$\frac{1}{231}$	$-\frac{2k_BT}{5eV}$

with

$$s = \frac{1}{3} + \frac{2\left(q_L^3 + q_R^3\right)}{3\left(1 + q_L + q_R\right)^3}. \tag{35}$$

The well known noise power of double tunnel barriers [1,49,50] and diffusive media [22,27,44–48] are recovered in the large and small q_L, q_R limits. The third Fano factor is found to be:

$$F_3 = \frac{K_3}{K_1} = 1 + \frac{k_BT}{eV} 3\left(s - 1 - 2f\right)\coth\left(\frac{eV}{2k_BT}\right) + \frac{f - 3(s-1)/2 + 2f\left[\cosh(\frac{eV}{2k_BT})\right]^2}{\left[\sinh(\frac{eV}{2k_BT})\right]^2} \tag{36}$$

with

$$f = -\frac{3}{10} + 3s\left(s - 1/2\right) - \frac{6(q_L^5 + q_R^5)}{5(1 + q_L + q_R)^5} \tag{37}$$

Equation (36) bridges continuously between two simple situations: double tunnel barriers (large q_L, q_R) and diffusive media (small q_L, q_R) for which we also recover known results [17,23]. In the low and high temperature limits, we found:

$$\begin{aligned} F_3(eV \gg k_BT) &= 1 + 2f \\ F_3(eV \ll k_BT) &= s = F(eV \gg k_BT). \end{aligned} \tag{38}$$

The high temperature skewness is equal to the low temperature noise power, as would be expected from a fully quantum treatment (see Eq. (21)).

3.4 Diffusive medium

In this section, we consider a diffusive medium with good contacts to the electrodes.

We first consider the SSEP model in the $N \to \infty$ limit, which is enough to account for a purely diffusive behavior. At the end of this section, we consider the cross-over from a ballistic to diffusive conduction. To do so, the counter-flows model will be required.

SSEP diffusive medium

In our previous paper [2], we detail the derivation of the FCS for SSEP models in the $N \to \infty$ limit and we shall only summarize the results here. The cumulant generating function $\mathcal{S}_t$ depends on N, z, ρ_L and ρ_R but to first order in $1/N$, $\mathcal{S}_t$ turns out to depend only on a combination ω of these parameters:

$$\omega = \frac{(z-1)(\rho_L z - \rho_R - \rho_L\rho_R(z-1))}{z}. \tag{39}$$

Consequently, to first order in $1/N$ one can write:

$$\mathcal{S}_t/t = \frac{\Gamma}{N} R(\omega) \tag{40}$$

where the expression of $R(\omega)$ has been conjectured. Thus, if the FCS is known for two arbitrary fillings of the electrodes, then it can be deduced for any fillings or at any temperature.

Based on the exact derivation of the first 4 cumulants, we conjectured that for $\rho_L = \rho_R = 1/2$, the statistics of current fluctuations is Gaussian (at order $1/N$). This fully determines $R(\omega)$ and thus the current statistics at a arbitrary fillings ρ_L and ρ_R:

$$\mathcal{S}_t/t = \frac{\Gamma}{N}\left[\log(\sqrt{1+\omega} + \sqrt{\omega})\right]^2. \tag{41}$$

This expression is identical to the one found at zero temperature by [15] and at arbitrary temperature by [17] (and by [51] with minor discrepancies). Table 2 gives the first cumulants C_n, K_n/K_1 for $k_BT \ll eV$ and for $k_BT \gg eV$. Right/Left symmetry and particle/hole symmetry suggest the change of parameters: $X = (\rho_L - \rho_R)$ and $Y = (\rho_L + \rho_R - 1)$. Agreement is found with the first four cumulants which can be easily derived from [23] (after correcting a typo: the last x in equation (24) should be an x_1).

Ballistic-diffusive cross-over

We now consider a counter-flows model with uniform symmetrical transmission coefficients Γ in the bulk of the conductor ($\Gamma = \Gamma_i^{(\rightarrow)} = \Gamma_i^{(\leftarrow)}$ for $1 < i < N+1$), unity

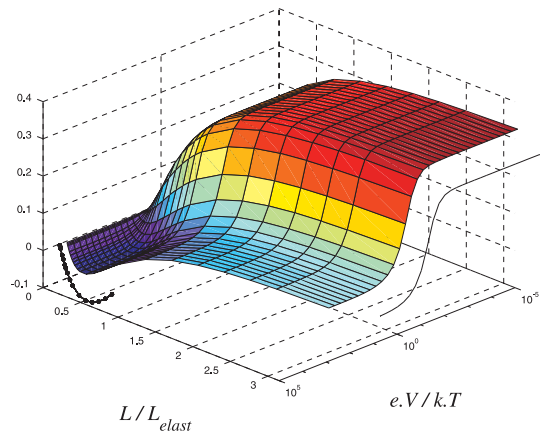

Fig. 9. Third Fano factor K_3/K_1 in a ballistic/diffusive medium parametrized by the ratio L/L_{elast} of the conductor's length L over a elastic mean free path L_{elast} (counter-flows with $N = 8$). The two lines correspond to known limit for $L/L_{elast} \gg 1$ (continuous line) and for $L/L_{elast} \ll 1$ with $eV \gg k_BT$ (pearly line).

transmission at the boundaries ($\Gamma_1^{(\leftarrow)} = \Gamma_1^{(\rightarrow)} = \Gamma_{N+1}^{(\leftarrow)} = \Gamma_{N+1}^{(\rightarrow)} = 1$), and we consider the $N \to \infty$ limit taken at constant $(1-\Gamma)(N-1)$. We can define the mean free path L_{elast} of a single electron as $1/(1-\Gamma)$ and the length L of the conductor as $N-1$. Then $(1-\Gamma)(N-1) = L/L_{elast} \ll 1$ corresponds to a ballistic conductor while $L/L_{elast} \gg 1$ to a diffusive one [28,52]. We explore the third Fano factor $F_3 = K_3/K_1$ versus both the ballistic-diffusive cross-over and the thermal ($k_BT \gg eV$) - shot noise ($eV \gg k_BT$) cross-over. At zero temperature, it was shown [26] that N as small as 8 gives a correct picture of the skewness, even in the diffusive limit. We performed a numerical simulation of such a small N by solving numerically the largest eigenvalue of the counting matrix. Figure 9 shows $F_3(L/L_{elast}, eV/k_BT)$. For comparison, the continuous line is calculated from the analytical results in the diffusive limit and good agreement is found with the numerical estimation. This is an interesting result, which shows a tendency of the simple exclusion model to reproduce the same FCS as for a larger class of models. This raises the question of trying to identify more precisely the key features which are required for a stochastic model to yield this FCS. The pearly line corresponds to a single scatterer with the same conductance as the system in the low temperature limit. As $L/L_{elast} \to 0$ (L may be arbitrary large), the system is expected to converge to such a point scatterer limit and a good agreement is found with the simulation. Good agreement is also found with Monte-Carlo simulations performed along the ballistic-diffusive cross-over at zero temperature [26].

4 Concluding remarks

In this paper, we have checked explicitly that the FCS of purely classical stochastic models with a local exclusion constraint coincides with the FCS of a large class of quantum mechanical microscopic models where the current flows between two reservoirs. In particular, no restriction on the system size seems to be necessary, since this coincidence appears for a small number of tunnel barriers, as well as in the limit of a diffusive medium composed of an arbitrary large number of such barriers. The two key common ingredients to both types of models are the stochastic nature of scattering processes and the constraint removing doubly occupied sites, imposed by the Pauli principle. The first ingredient establishes a very interesting difference between classical Hamiltonian mechanics, where diffusion is a chaotic but deterministic process, and quantum mechanics, where an intrinsic notion of probability arises. This distinction is the same as the difference between ray and wave optics. As shown in [53], the crossover from the first regime to the second occurs when the typical time spent by a wave-packet in the system becomes larger than the Ehrenfest time associated to the spreading of this wave-packet induced by the underlying chaotic dynamics. Our stochastic models require physical systems dominated by diffractive scattering.

This work raises the question of the role of space dimensionality in the FCS of classical exclusion models. It would also be very interesting to extend the classical approach in terms of exclusion models to multi-terminal geometries. Such generalizations have been considered in a fully quantum-mechanical treatment of diffusive systems [47], or in the semi-classical Boltzmann-Langevin approach [48]. These works have so far focused on the correlation matrix of the integrated charges flowing through each contact during a finite time interval. A natural question is whether simple classical exclusion models are able to generate these results for the second order cumulants. The computation of higher-order cumulants in multi-terminal geometries is another interesting open question.

5 Appendix: Quantum treatment of a double barrier

We consider here the quantum version of the calculation for a double barrier of Section 3.2, but adapted to the case where transmissions $\mathcal{T}_1$, $\mathcal{T}_2$ are not assumed to be small. Our starting point is the composition rule for the series of two barriers:

$$t = \frac{t_1 t_2}{1 - r_1' r_2} = \frac{t_1 t_2}{1 - |r_1||r_2|e^{i\phi}} \tag{42}$$

where $\mathcal{T}_i = |t_i|^2$, and $|t_i|^2 + |r_i|^2 = 1$. We have seen that when both $\mathcal{T}_1$ and $\mathcal{T}_2$ are small, integrating over the phase ϕ of $r_1' r_2$ with a uniform weight yields the FCS of the counter-flows model, in the limit where $\Gamma_1, \Gamma_2 \ll 1$, which coincides with the FCS of the Symmetric Simple Exclusion Model for a double barrier. This integration over the phase-shift ϕ is motivated in this case by the fact that $|t|^2$ exhibits a sharp resonance as a function of ϕ. So even for a single coherent channel, a rather small voltage drop induces an energy spread for the incoming electrons which

is larger than the energy width of the resonance, thereby justifying the ϕ integration.

When $\mathcal{T}_i$'s are no longer small, $|t(\phi)|$ becomes a rather smooth function of ϕ, and resonances tend to disappear, since the inner regions between the barriers is now well coupled to reservoirs. For a single channel, averaging over ϕ takes place only if:

$$eV \gg \frac{\hbar^2 k_{\mathrm{F}}}{ml}. \tag{43}$$

For smaller voltages, the FCS becomes a binomial law obtained by the quantum series composition rule equation (42), where the phase-shift is taken at the Fermi level. In this case, it is clear that the FCS of the counter-flows model given by equation (23) does not agree with the full quantum treatment, since the former has lost all information on phases of reflection coefficients.

What happens in a situation where ϕ-averaging makes sense? Besides the single channel case, in the regime of equation (43), we have in mind a coherent system with a large number of transverse conduction channels. For a given value of the total single particle energy, a large spread in the longitudinal wave-vector $k_\parallel$ is obtained by varying its transverse component $k_\perp$. We assume clean interfaces, with no disorder along the barrier so that the potential seen by electrons may be decomposed as a sum $V(\mathbf{r}) = V(\mathbf{r}_\parallel) + V(\mathbf{r}_\perp)$. For this reason, the system we consider is quite different from the chaotic cavity studied in references [1,25]. The scattering matrix of such system is diagonal in the same basis as for the conduction channels of the reservoirs, and we neglect any dependency of coefficients r_i, t_i on the longitudinal wave-vector $k_\parallel$. The phase entering in expression (42) is then equal to $2k_\parallel l$. The FCS is given by:

$$\mathcal{S}_t(z)/t = \frac{eV}{h} N_\perp \frac{1}{2\pi i} \times \oint \frac{du}{u} \ln\left(1 + \frac{\mathcal{T}_1\mathcal{T}_2}{1 + \mathcal{R}_1\mathcal{R}_2 - \sqrt{\mathcal{R}_1\mathcal{R}_2}(u + u^{-1})}(z-1)\right) \tag{44}$$

where $u \equiv e^{i\phi}$, $N_\perp$ is the number of transverse conduction channels, and the integral is along the unit circle in the complex plane.

When z is real and larger than 1, the logarithm in this integral exhibits a branch cut along the interval $[u_1, u_2]$ illustrated on Figure 10, with:

$$u_1 = \frac{a - \sqrt{a^2 - 4}}{2}, \quad a = \frac{2b(z)}{\sqrt{\mathcal{R}_1\mathcal{R}_2}} \tag{45}$$

$$u_2 = \sqrt{\mathcal{R}_1\mathcal{R}_2} \tag{46}$$

We have defined $b(z)$ as:

$$b(z) = \frac{1 + \mathcal{R}_1\mathcal{R}_2 + \mathcal{T}_1\mathcal{T}_2(z-1)}{2}. \tag{47}$$

Note that the pole at $u = 0$ turns out to have a vanishing residue.

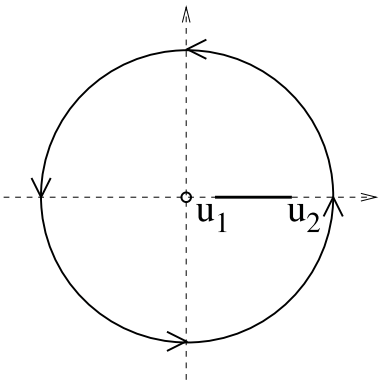

Fig. 10. Location of the branch cut singularity in the complex u plane, while computing integral (44). This analytic structure corresponds to the case where z is real and larger than 1.

We find then:

$$\mathcal{S}_t(z)/t = \frac{eV}{h} N_\perp \log\left(\frac{u_2}{u_1}\right), \tag{48}$$

and finally:

$$\mathcal{S}_t(z)/t = \frac{eV}{h} N_\perp \log\left(b(z) + \sqrt{b(z)^2 - \mathcal{R}_1\mathcal{R}_2}\right), \tag{49}$$

which is exactly proportional to the result equation (23) obtained for the FCS of the counter-flows model.

References

1. Y.M. Blanter, M. Büttiker, Phys. Rep. **336**, 1 (2000)
2. B. Derrida, B. Douçot, P.-E. Roche, J. Stat. Phys. **115**, 717 (2004)
3. L.S. Levitov, H.-W. Lee, G.B. Lesovik, J. Math. Phys. **37**, 4845 (1996)
4. H. Spohn, *Large scale dynamics of interacting particles* (Springer Verlag, Berlin, 1991)
5. B. Derrida, J.L. Lebowitz, E.R. Speer, Phys. Rev. Lett. **87**, 150601 (2001)
6. T.M. Liggett, *Stochastic interacting systems: contact, voter and exclusion processes* (Springer Verlag, New-York, 1999)
7. V.A. Khlus, Zh. Eksp. Teor. Fiz. **93**, 2179 (1987) [Sov. Phys. JETP **66**, 1243 (1987)]
8. G.B. Lesovik, Pis'ma Zh. Eksp. Teor. Fiz **49**, 592–4 (1989) [JETP Lett. **49**, 513-5 (1989)]
9. M. Büttiker, Phys. Rev. Lett. **65**, 2901 (1990)
10. A. Shimizu, H. Sakaki. Phys. Rev. B **44**, 13136–9 (1991)
11. M. Büttiker, Phys. Rev. B **46** (19), 12485 (1992)
12. L.S. Levitov, G.B. Lesovik, Pis'ma Zh. Eksp. Teor. Fiz. **58**, 225 (1993) [JETP Lett. **58**, 230-5 (1993)]
13. B.A. Muzykantskii, D.E. Khmelnitskii, Phys. Rev. B **50**, 3982 (1994)
14. C.W.J. Beenakker, Rev. Mod. Phys. **69**, 731 (1997)
15. H. Lee, L.S. Levitov, A.Yu. Yakovets, Phys. Rev. B **51**(7), 4079 (1995)
16. L.V. Keldysh, L.V. Keldysh, Zh. Eksp. Teor. Fiz. **47**, 1515 (1964) [JETP **20**, 1018 (1965)]

17. D.B. Gutman, Y. Gefen, A.D. Mirlin, in *Quantum Noise in Mesoscopic Physics*, edited by Y.V. Nazarov, pages 497−524 (Kluwer Academic Publishers, Dordreicht, 2003), pp. 497–524
18. Y.V. Nazarov, in *Quantum dynamics of submicron structures*, edited by H. Cerdeira, B. Kramer, G. Schoen, 1995, p. 687
19. Y.V. Nazarov, D.A. Bagrets, Phys. Rev. Lett. **88**, 196801 (2002)
20. A.Ya. Shulman, Sh.M. Kogan, Zh. Eksp. Teor. Fiz. **57**, 2112 (1969) [Sov. Phys. JETP **29**, 3 (1969)]
21. S.V. Gantsevich, V.L. Gurevich, R. Katilius, Sov. Phys. JETP **30**, 276 (1970)
22. K.E. Nagaev, Phys. Lett. A **169**, 103 (1992)
23. K.E. Nagaev, Phys. Rev. B **66**, 075334 (2002)
24. M.J.M. de Jong, Phys. Rev. B **54**, 8144 (1996)
25. S. Pilgram, A.N. Jordan, E.V. Sukhorukov, M. Büttiker, Phys. Rev. Lett. **90**, 206801 (2003)
26. P.-E. Roche, B. Douçot, Eur. Phys. J. B **27**, 393 (2002)
27. M.J.M. de Jong, C.W.J. Beenakker, Phys. Rev. B **51**, 16867 (1995)
28. R.C. Liu, P. Eastman, Y. Yamamoto, Solid. State Comm. **102**, 785 (1997)
29. B. Yurke, G.P. Kochanski, Phys. Rev. B **41**, 8184 (1990)
30. R. Landauer, T. Martin, Physica B **175**, 167 (1991)
31. M. Reznikov, M. Heiblum, H. Shtrikman, D. Mahalu, Phys. Rev. Lett. **75**, 3340 (1995)
32. A. Kumar, L. Saminadayar, D.C. Glattli, Phys. Rev. Lett. **76**, 2778 (1996)
33. H. Spohn, J. Phys. A **16**, 4275 (1983)
34. B. Derrida, J.L. Lebowitz, Phys. Rev. Lett. **80**, 209 (1998)
35. L.S. Levitov, M. Reznikov, `cond-mat/0111057`, 2001 (see also Phys. Rev. B **70**, 115305 (2004))
36. D.B. Gutman, Y. Gefen, Phys. Rev. B **68**, 035302 (2003)
37. B. Reulet, J. Senzier, D.E. Prober, Phys. Rev. Lett. **91**, 196601 (2003)
38. D.A. Bagrets, Y.V. Nazarov, Phys. Rev. B **67**, 085316 (2003)
39. W. Belzig, in *Quantum Noise in Mesoscopic Physics*, edited by Y.V. Nazarov (Kluwer Academic Publishers, Netherlands, 2003), pp. 469–496
40. A.K. Savchenko, S.S. Safonov, S.H. Roshko, D.A. Bagrets, O.N. Jouravlev, Y.V. Nazarov, E.H. Linfield, D.A. Ritchie, Physica Status Solidi (b) **241**, 26 (2004)
41. L.I. Glazman, K.A. Matveev, Pis'ma Zh. Eksp. Teor. Fiz. **48**, 403 (1988) [JETP Lett. **48**, 445 (1988)]
42. S. Hershfield, J.H. Davies, P. Hyldgaard, C.J. Stanton, J.W. Wilkins, Phys. Rev. B **47**, 1967 (1993)
43. Y.A. Kinkhabwala, A.N Korotkov, Phys. Rev. B **62**, R7727 (2000)
44. C.W.J. Beenakker, M. Büttiker, Phys. Rev. B **46**, 1889 (1992)
45. Y.V. Nazarov, Phys. Rev. Lett. **73**(1), 134 (1994)
46. B.L. Al'tshuler, L.S. Levitov, A.Yu. Yakovets, Pis'ma Zh. Eksp. Teor. Fiz. **59**, 821 (1994) [JETP Lett. **59**, 857 (1994)]
47. Y.M. Blanter, M. Büttiker, Phys. Rev. B **56**, 2127 (1997)
48. E.V. Sukhorukov, D. Loss, Phys. Rev. Lett. **80**, 4959 (1998)
49. L.Y. Chen, C.S. Ting, Phys. Rev. B **43**, 4534 (1991)
50. J.H. Davies, P. Hyldgaard, S. Hershfield, J.W. Wilkins, Phys. Rev. B **46**, 9620 (1992)
51. Y.V. Nazarov, Ann. Phys (Leipzig) **8**, Spec. Issue SI-**193**, 507 (1999)
52. M.J.M. de Jong, C.W.J. Beenakker, in *Mesoscopic electron transport*, edited by L.P. Kouwenhoven, G. Schön, L.L. Sohn, Vol. 345 of NATO Advances Studies Institute (ASI) Series E: Applied Sciences (Kluwer Academic Plublishers, Dordrecht, 1996)
53. O. Agam, I. Aleiner, A. Larkin, Phys. Rev. Lett. **85**, 3153 (2000)